JOURNAL OF CATALYSIS **151**, 204–215 (1995)

The Activation of Hydrocarbon C–H Bonds over Transition Metal Oxide Catalysts: A FTIR Study of Hydrocarbon Catalytic Combustion over $MgCr_2O_4$

Elisabetta Finocchio,* Guido Busca,* Vincenzo Lorenzelli,* and Ronald J. Willey†

**Istituto di Chimica, Facoltà di Ingegneria, Università, P.le Kennedy, I-16129 Genova, Italy; and †Department of Chemical Engineering, Northeastern University, Boston, Massachusetts 02115*

Received June 7, 1994; revised August 31, 1994

The interaction of light hydrocarbons (methane, ethane, propane, propene, *n*-butane, isobutane, 1-butene, benzene, and toluene) with the oxidized surface of the spinel $MgCr_2O_4$ (an active hydrocarbon combustion catalyst) has been investigated by FTIR spectroscopy in the temperature range 300–773 K. This interaction results in the reduction of the catalyst and the production of oxygen-containing adsorbed species. These species have been identified by comparison with the spectra of oxygen-containing species (alcohols, aldehydes, ketones, carboxylic acids, carbon oxides) directly adsorbed on the surface. It has been concluded that every hydrocarbon reacts at its weakest C–H bond on $Cr^{n+}{=}O$ (n = 5 or 6) surface sites giving rise by hydrogen abstraction and C–O bond formation to alkoxy groups. These species are further oxidized to carbonyl compounds and/or carboxylate anions and, finally, carbon oxides. The earlier intermediates (alkoxides, carbonyl compounds) are detectable only with the most reactive hydrocarbons (propane, *n*-butane, isobutane, propene, 1-butene, toluene) while with the least reactive hydrocarbons (methane and benzene), because of their too high activation temperature, only the final intermediates are detectable (carbonates, carboxylates). Molecular-level mechanisms for C–H cleavage and hydrocarbon catalytic combustion are proposed. © 1995 Academic Press, Inc.

INTRODUCTION

The catalytic partial oxidation processes of olefins and aromatics represent a prominent area of petrochemistry (1, 2). Recently, the use of light alkanes for the direct production of oxygenates via partial oxidation or for the production of olefins via dehydrogenation or oxidative dehydrogenation has become more and more attractive because of the large availability and low price of natural gas (3). On the other hand, attention is also focused on the catalytic combustion of hydrocarbons in developing new processes aimed to a limitation of air pollution (4, 5). Most of the above-mentioned partial oxidation processes are performed using transition metal oxides as heterogeneous catalysts. In the case of catalytic combustion, however, the possibility of using transition metal oxide catalysts, much cheaper than noble metal-based catalysts, is doubtful although hopeful.

In spite of the great interest in these processes, partially conflicting opinions are reported in the literature concerning several details of the mechanisms of partial oxidation over oxide catalysts. Even much less is known on combustion catalysis, according to Spivey (5). Among the points still under discussion we can cite: (i) the reaction scheme for total and partial oxidation; i.e., whether total oxidation is competitive or successive to partial oxidation; (ii) the nature of the oxygen active species (e.g., nucleophilic and electrophilic oxygen) in partial and total oxidation; (iii) whether activation of the hydrocarbon in the case of catalytic combustion is needed; (iv) the configuration of the active sites and the mechanism for C–H activation towards partial oxidation; (v) the configuration of the active sites for C–H activation towards total oxidation, if this activation is needed; (v) the role and the nature of adsorbed and gas-phase partially oxidized intermediates in total oxidation.

We recently undertook (6) a research program on alkane oxidation mechanisms at metal oxide surfaces, using FTIR spectroscopy. In the present paper we report our data on the activation of a number of hydrocarbons on an $MgCr_2O_4$ aerogel. The catalytic activity of this material in the combustion of propane and propene has also been investigated in a flow reactor, confirming that $MgCr_2O_4$ is an efficient combustion catalyst, as reported by Margolis several years ago for ethylene, propene, *n*-alkanes, and benzene (7). So, $MgCr_2O_4$ has been taken as a model of transition metal-oxide combustion catalysts of the chromite type, like α-Cr_2O_3 (8), $CuCr_2O_4$ (7, 9), $ZnCr_2O_4$ (9), and $LaCrO_3$ (10)). In spite of the unlikely substitution of noble metal catalysts by transition metal catalysts for combustion purposes, the possibility of hydrocarbon catalytic combustion over transition metal oxides like chromites has been studied in recent years (5) and can additionally give information in order to limit nonselective processes upon selective oxidation. The aim

0021-9517/95 $6.00

of this work is to obtain additional information on the above-cited still incompletely clarified topics.

EXPERIMENTAL

The preparation and the solid state and surface characterization of the $MgCr_2O_4$ aerogel (53 m^2/g) have been described previously (6, 11). XRD and FT–FIR analyses show that the sample after activation consists of the spinel-type phase $MgCr_2O_4$, very well crystallized, although with excess oxygen at the surface.

FTIR spectra have been recorded with a Nicolet Magna 750 instrument, using conventional IR cells connected with evacuation-gas manipulation apparatus. The pure catalyst powder was pressed into self-supporting disks that were calcined at 723 K for 2 h and later outgassed at the same temperature for 1 h before adsorption experiments. The threshold oxidation temperature of the different hydrocarbons has been measured as the temperature at which oxidized surface species become detectable upon contact of the catalyst with the hydrocarbon gas.

Catalytic activity in propane and propene oxidation was measured with a 1-cm i.d. pyrex glass U-tube reactor charged with 0.1 g of the catalyst, with He : hydrocarbon : oxygen mixtures 88 : 2 : 10 at a total flow rate of 100 cm^3/min. Product analysis was performed with a HP 5890 gas cromatograph. Liquid adsorbates were from Carlo Erba (Milano, Italy), while gases were purchased from SIO (Milano, Italy).

RESULTS

In Fig. 1 the "light-off" curves relative to propene and propane oxidation over our $MgCr_2O_4$ aerogel catalyst are shown. No products different from carbon oxides and water were observed under these conditions. In spite of the limits of this kind of representation of catalytic combustion activity, underlined recently by Hubbard *et al.* (12), these data unequivocally show that our catalyst is active in hydrocarbon combustion in the same temperature range of other chromite catalysts (7–10) as well as of other transition metal oxides like, for example, $LaCoO_3$ (13); however, it is less active than noble metal-based combustion catalysts (12, 14). A more detailed study of hydrocarbons combustion over this catalyst in a flow reactor is now in progress.

In Fig. 2a the FTIR spectrum of an activated pressed disk of the catalyst is shown. It presents a complex series of absorptions in the region between 1010 and 800 cm^{-1} and is completely opaque below 800 cm^{-1}. This cutoff is due to the lattice vibrations of the $MgCr_2O_4$ spinel-type phase. The complex absorption at higher frequencies is associated to the Cr=O stretching modes of chromate species involving higher valency chromium species (most probably Cr^{6+}, although a participation of Cr^{5+} is not excluded, as proposed by Klissurski *et al.* (15) for α-Cr_2O_3). This excess oxygen at the surface gives rise to *p*-type semiconducting $MgCr_2O_{4+x}$ (11, 16). Accordingly, these absorptions completely disappear by reduction treatments, e.g., with hydrogen (11) or organic compounds,

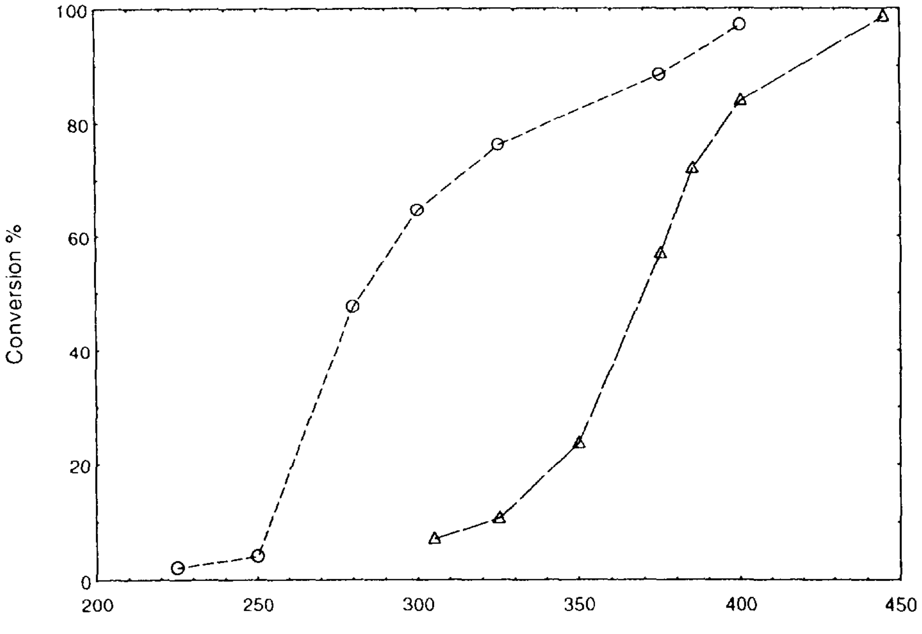

FIG. 1. Conversion of propene (circles) and propane (triangles) as a function of temperature over $MgCr_2O_4$ aerogel catalyst.

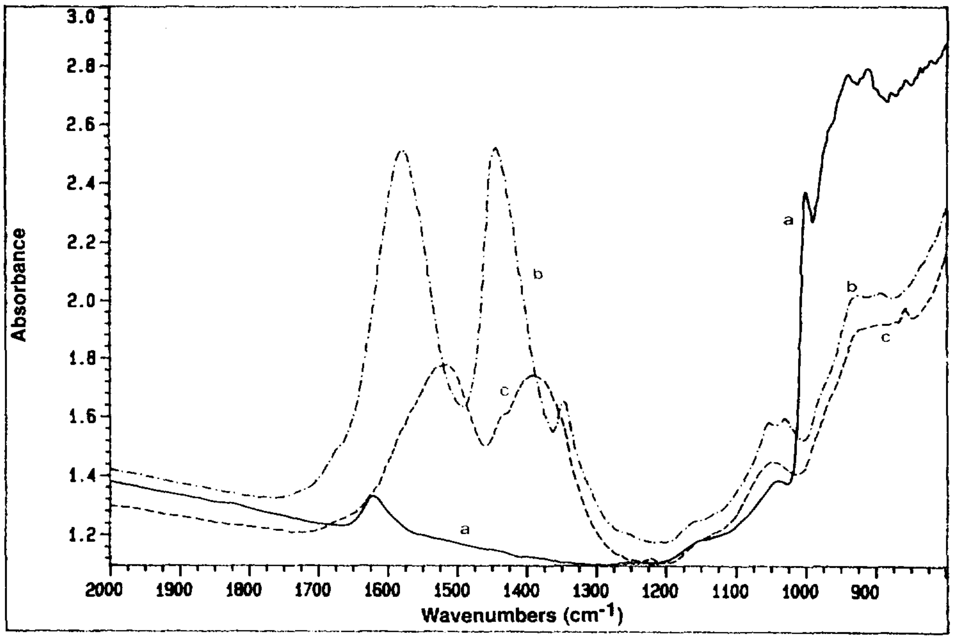

FIG. 2. FTIR spectra of the oxidized $MgCr_2O_{4+x}$ catalyst disk after activation (a), and after following interaction with acetaldehyde gas and outgassing at 623 (b) and 773 K (c).

that produce stoichiometric $MgCr_2O_4$. This is shown in Fig. 2b after contact of the catalyst with acetaldehyde vapour (1 Torr) at 623 K. The aldehyde burns in part and in part remains adsorbed on the catalyst surface in the form of acetate ions (bands near 1600, 1430, and 1350 cm^{-1}, in Fig. 2b, represent asymmetric and symmetric COO stretchings and CH_3 bending, respectively) and, simultaneously, the above-cited bands, associated to the oxidized catalyst surface sites, are eroded almost completely. Acetate species later are overoxidized to carbonates and gas-phase CO_2, in the temperature range 573–773 K.

So, the bands in the region 1010–800 cm^{-1}, present in the spectrum of the oxidized catalyst, but not in that of the stoichiometric "reduced" $MgCr_2O_4$ catalyst, allow us to monitor the oxidation state of the catalyst surface. These bands are reduced fast or completely by organic compounds (hydrocarbons and oxygenates) and hydrogen in the temperature range 573–773 K, but are also restored in this temperature range by contact with oxygen or air. This shows that in the range 573–773 K (at which $MgCr_2O_4$ acts as an efficient propane combustion catalyst, see Fig. 1) the catalyst redox cycles are fast. These data strongly suggest that: (i) the oxidation reactions we observe by IR and we will discuss below represent adequately what occurs upon catalytic combustion in flow reactor steps; (ii) these oxidation reactions occur at the expense of lattice oxygen of the oxidized surface that can be restored by air under the same conditions, thus implying a Mars–van Krevelen-type (redox) oxidation mechanism (17).

When the oxidized catalyst disk is put into contact with methane gas, the spectrum of the catalyst is not modified at all up to 773 K, showing that reaction does not occur below this temperature. At 773 K an interaction occurs, shown by the decrease of the absorptions in the region 1010–800 cm^{-1} (shown as negative bands in the subtraction spectrum in Fig. 3), by the detection of gas-phase CO_2 (band at 2340 cm^{-1} with the typical PR rotovibrational contour), and, finally, by the detection of new absorption bands associated to adsorbed species. These bands (Fig. 3) are found at 1630 cm^{-1} (with a shoulder near 1610 cm^{-1}), 1520, 1405, and 1222 cm^{-1}; the last one is very weak. According to the detection of gas-phase CO_2, the bands at 1520 and 1405 cm^{-1} can be assigned to surface carbonate species, probably of the bidentate type, while those at 1610 and 1222 cm^{-1} (together with a further component masked near 1450 cm^{-1}) can be assigned to bicarbonate ions (18). The band at 1630 cm^{-1} is associated to adsorbed water, responsible also for a broad absorption in the region 3500–3000 cm^{-1}. From these data we conclude that methane molecules can burn by reaction with the surface. This reaction is observed at 773 K, and, under these conditions, only the final products of these reactions are observed; i.e., CO_2, carbonates, water, and the reduced catalyst.

If contact of the activated catalyst with ethane gas is carried out, the reaction is observed at much lower tem-

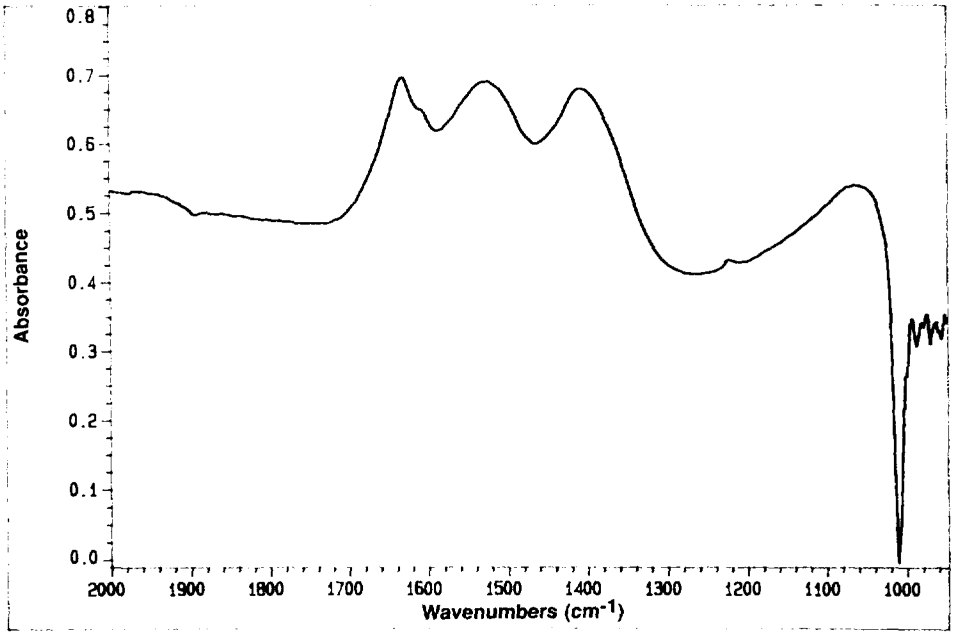

FIG. 3. FTIR spectrum of the species arising from methane oxidation over $MgCr_2O_{4+x}$ and successive evacuation at 773 K. The spectrum of the activated catalyst disk has been automatically subtracted.

perature (Fig. 4). With 150 Torr of ethane gas the formation of adsorbed species and the erosion of the bands associated to chromate species are observed already at 423 K. The most intense bands due to adsorbed species are observed at 1600 and 1440 cm^{-1}. These features, together with a weaker component at 1350 cm^{-1}, closely correspond to those of acetate species, either produced by acetic acid adsorption or, alternatively, by ethanol and acetaldhyde oxidation on the same surface (compare with Fig. 2). A weak band at 1385 cm^{-1} and a shoulder near

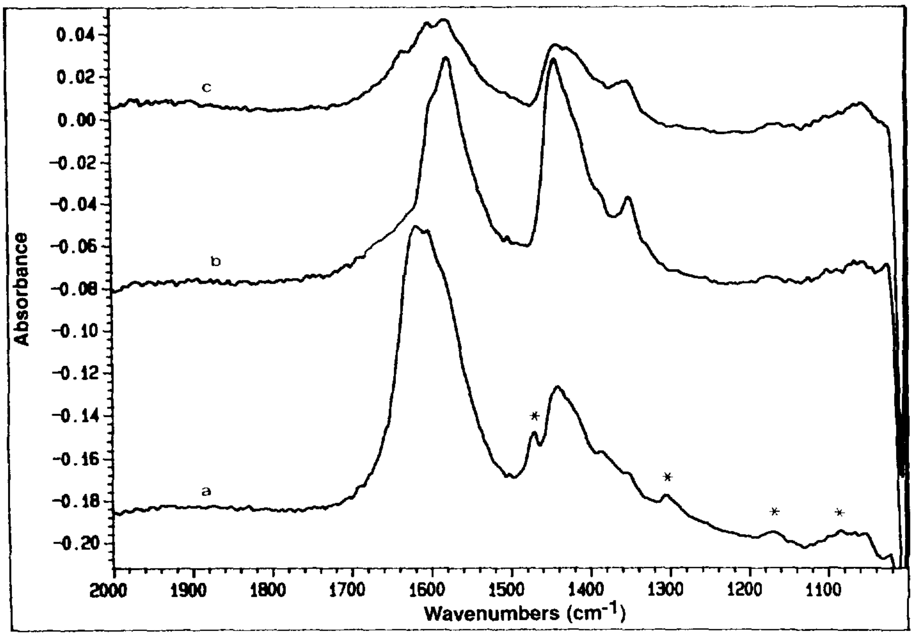

FIG. 4. FTIR spectra of the species arising from ethane oxidation over $MgCr_2O_{4+x}$ and successive evacuation at 423 (a), 523 (b), and 573 K (c). The spectrum of the activated catalyst disk has been automatically subtracted. (*) Bands due to adsorbed acetaldehyde.

1580 cm^{-1} could be associated to traces of formate ions (asymmetric and symmetric COO stretchings) produced by deeper oxidation. The identification, in this case and in the following ones, of carboxylate species has been confirmed by the analysis of the spectra of these species produced by dissociative adsorption of the corresponding acids (formic, acetic, propionic, acrylic, butirric, methacrylic, crotonic acids (6)). Other sharp peaks at 1470 and 1304 cm^{-1}, together with broad and stronger absorptions centered near 1180 and 1060 cm^{-1}, can tentatively be assigned to dioxy-ethylydene species $-O-(CH_3)CH-O-$, an adsorbed form of acetaldehyde similar to dioxy-methylene $-O-CH_2-O-$ species produced by formaldehyde adsorption and widely described previously (19).

With further heating the last adsorbed species disappear. Acetate species burn on this surface in the temperature range 573–773 K, giving rise to CO_2 and water, and completely reduce the catalyst surface. These data indicate that ethane catalytic combustion on this surface occurs with the intermediacy of acetate species, which later undergo further oxidation up to carbon oxides. However, acetaldehyde is likely an earlier intermediate.

Interaction between the activated catalyst surface and higher alkanes, like propane, *n*-butane, and isobutane, is observed to occur in the temperature range 373–423 K. The interaction of propane with this catalyst has been the object of a previous detailed study (6). The surface species produced by this interaction (Fig. 5a) in the range 373–423 K are characterized by strong bands at 1590, 1440, 1385, and 1355 cm^{-1}, due to a mixture of acetate and formate species, while the weaker bands near 1700, 1240, and 1095 cm^{-1} are due to adsorbed acetone (Fig. 5b). This assignment is based on the comparison of these spectral features with those of any hydrocarbon or oxygenate adsorbed species that could be formed by propane oxidation and, in particular, of adsorbed acetone. These data support the idea that acetone is the primary detectable oxidation product of propane, which is later oxidized at C_1–C_2, giving rise to a mixture of formates and acetates that later produce carbon oxides as final products.

A strictly similar situation is found for *n*-butane interaction with the surface of oxidized $MgCr_2O_{4+x}$ (Fig. 6). Also in this case the strongest bands are observed near 1590, 1440, and 1355 cm^{-1} and can be assigned to acetate species. However, sharper bands near 1690, 1475 (very weak), 1385 (sharp and rather strong), and 1175 cm^{-1} are also found and all correspond to evident features in the spectrum of adsorbed methyl-ethyl ketone (C=O stretching, asymmetric and symmetric CH_3 bendings, and C–C–C asymmetric stretching, respectively), as shown in Fig. 6. A further sharp band at 1025 cm^{-1} could be associated, together with a broader absorption in the range 1150-1100 cm^{-1} to C–O and C–C Stretchings of 2-butoxy species, by comparison with the spectrum of adsorbed 2-butanol (Fig. 6c). The formation of *sec*-butoxy species from *n*-butane is also substantiated by the obser-

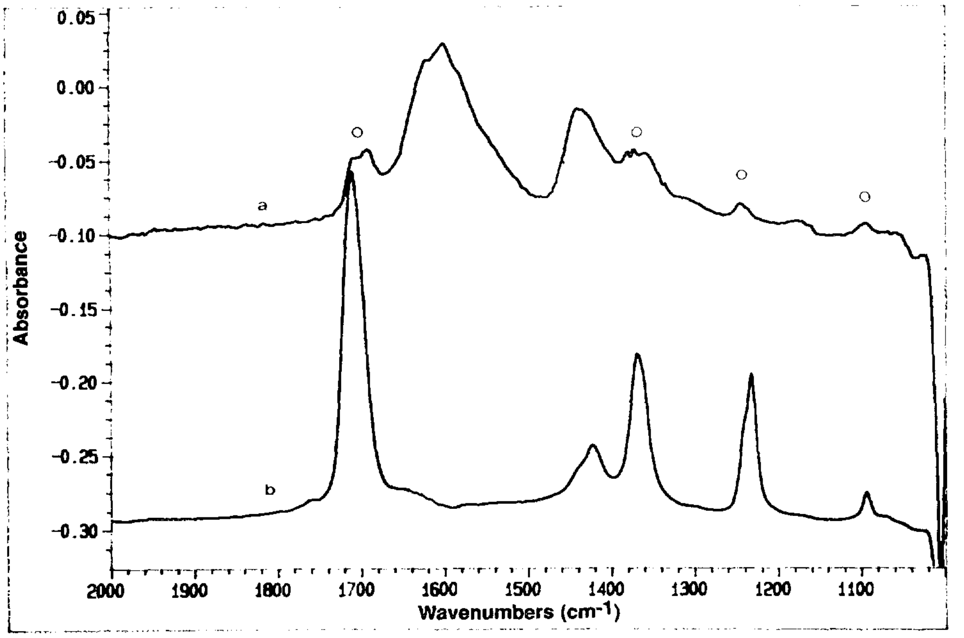

FIG. 5. FTIR spectra of the species arising from propane oxidation over $MgCr_2O_{4+x}$ at 423 K (a), and of the adsorbed acetone over the same surface at room temperature (b). The spectrum of the activated catalyst disk has been automatically subtracted. (○) Bands due to adsorbed acetone.

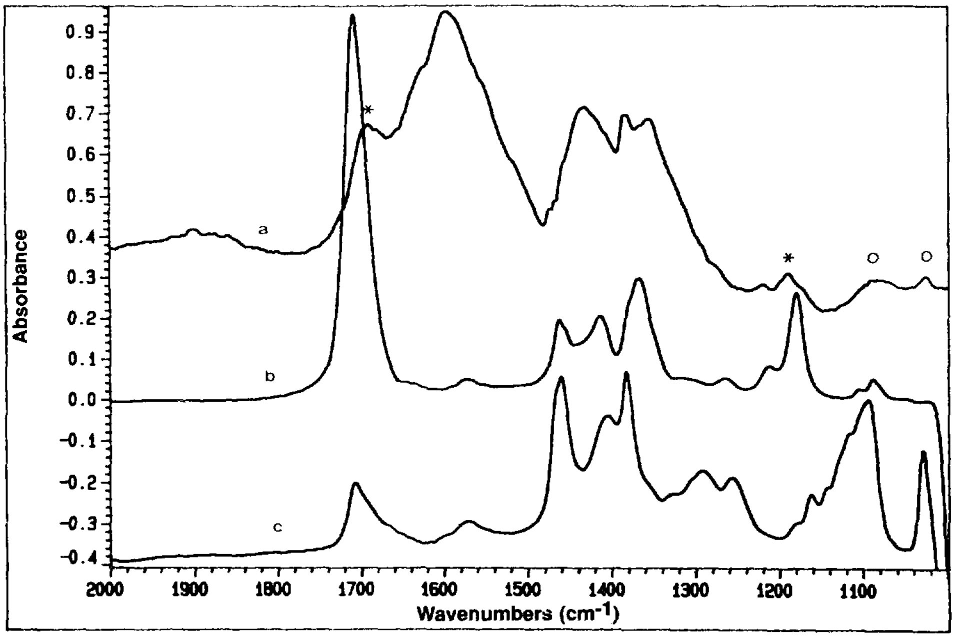

FIG. 6. FTIR spectrum of the species arising from *n*-butane oxidation over $MgCr_2O_{4+x}$ at 423 K (a); FTIR spectra of the adsorbed 2-butanone (metyl ethyl ketone) (b) and 2-butanol (c) over the same surface at room temperature. The spectrum of the activated catalyst disk has been automatically subtracted. (*) Bands due to adsorbed 2-butanone; (o) Bands due to adsorbed 2-butoxy-groups.

vation of the same spectra by oxidation of 2-butanol and *n*-butane at higher temperature on this surface, both giving acetate species by C_2–C_3 oxidative bond breaking.

So, while the interaction of methane only shows the final products of oxidation (carbon oxides and water) and that of ethane provides mainly evidence of a terminal intermediate species (acetates), the interaction of the more reactive C_3 and C_4 linear alkanes is more informative, giving definite evidence of earlier intermediates, i.e., the ketones acetone and methyl ethyl ketone. In the case of *n*-butane interaction the formation of an even earlier intermediate, 2-butoxide, can be suspected. To obtain more evidence of the very first stages in hydrocarbon activation, the interaction of isobutane, propylene, and 1-butene, expected to be even more reactive, has also been investigated.

The spectra of the adsorbed species arising from the interaction of isobutane with the surface of the catalyst at 373 K are shown in Fig. 7, where they are also compared with the spectra of adsorbed terbutanol. The most evident species formed by isobutane interaction with the catalyst surface are again formates (bands at 1590, 1385, and 1350 cm^{-1}), relatively more intense than in the previous cases, and acetate species (bands at 1560, 1430, and 1355 cm^{-1}, relatively less intense than in previous cases). This provides evidence of the oxidative breaking to two C–C bonds of isobutane, giving rise to two C_1 fragments (formates) and one C_2 fragment (acetates). However, weak but evident bands are also observed at 1245 and 1190 cm^{-1}. These bands are associated to C–C and C–O stretchings of *ter*-butoxide species (20, 21) and closely correspond to the bands produced by *ter*-butanol dissociative adsorption (Fig. 7c). It is remarkable that *ter*-butanol oxidation on our catalyst gives rise to the same bands produced also by isobutane, and assigned to acetate and formate species, with the same intensity ratios. This indicates that the C–H bond of isobutane is first broken and a C–O bond is formed, giving rise to *ter*-butoxide species. These species evolve by breaking of a C–C bond to formate and acetone, which, under the same conditions quickly transforms to acetate and formates. So, each isobutane molecule gives rise to two formate and one acetate species.

The spectra relative to the interaction of 1-butene with the catalyst (Fig. 8) provide definite evidence of the formation of adsorbed methyl vinyl ketone (bands at 1667, 1634, and 1173 cm^{-1}, due to $\nu C{=}O$, $\nu C{=}C$, and νC–C (22)) as the most evident product already at room temperature. A further band observed at 1019 cm^{-1}, due neither to 1-butene nor to methyl vinyl ketone, is likely associated to the C–O stretching of a 2-but-3en-oxide, analogous to the C–O stretching of allyl alcoholates. This result parallels that obtained by propene adsorption and oxidation on this surface studied previously (6) that showed acrolein and also allyl alcoholate species as the first products. However, allylic oxidation of 1-butene oc-

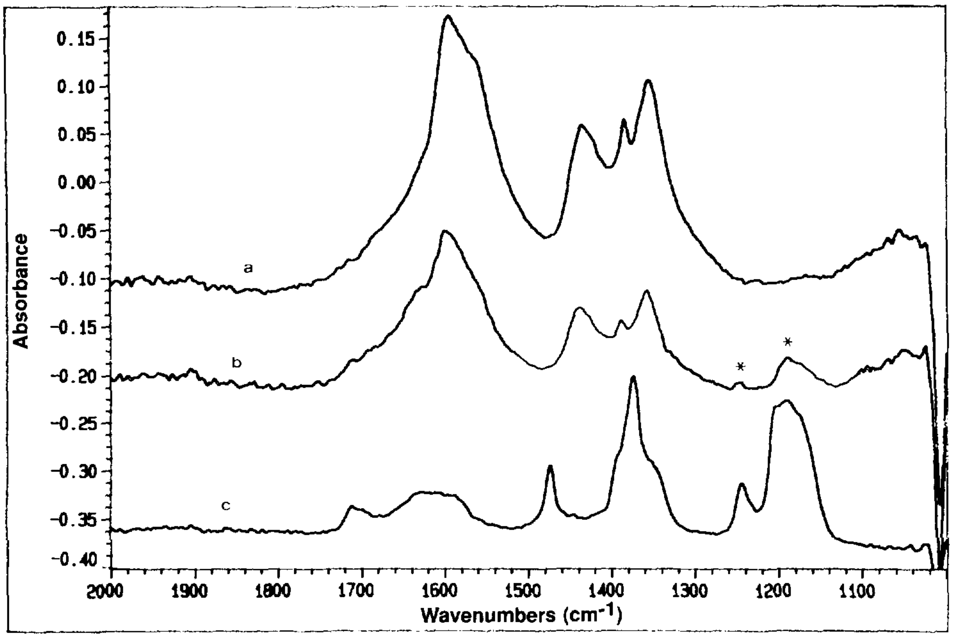

FIG. 7. FTIR spectra of the species arising from isobutane oxidation over $MgCr_2O_{4+x}$ and successive evacuation at 423 (a) and 323 K (b); FTIR spectrum of *ter*-butanol adsorbed at room temperature over the same surface (c). The spectrum of the activated catalyst disk has been automatically subtracted. (*) Bands due to adsorbed terbutoxy-groups.

curs apparently even faster than that of propene, being observed already at room temperature, instead of near 373 K.

In Fig. 9 the spectra of the adsorbed species arising from the oxidation of benzene and toluene on the surface of $MgCr_2O_{4+x}$ are reported. Benzene oxidation is detectable only above 573 K, giving rise to carboxylate species, certainly arising from the oxidative breaking of the aromatic ring. The oxidation of toluene is much faster, being observed already near 423 K, but being very fast at 473

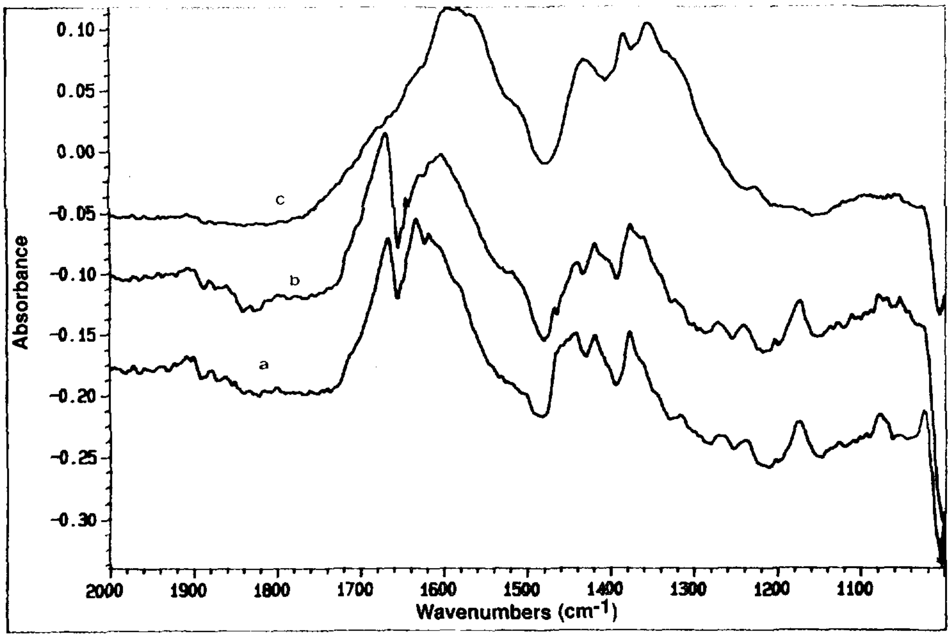

FIG. 8. FTIR spectra of the species arising from 1-butene oxidation over $MgCr_2O_{4-x}$ and successive evacuation at 300 (a), 373 (b), and 573 K (c). The spectrum of the activated catalyst disk has been automatically subtracted.

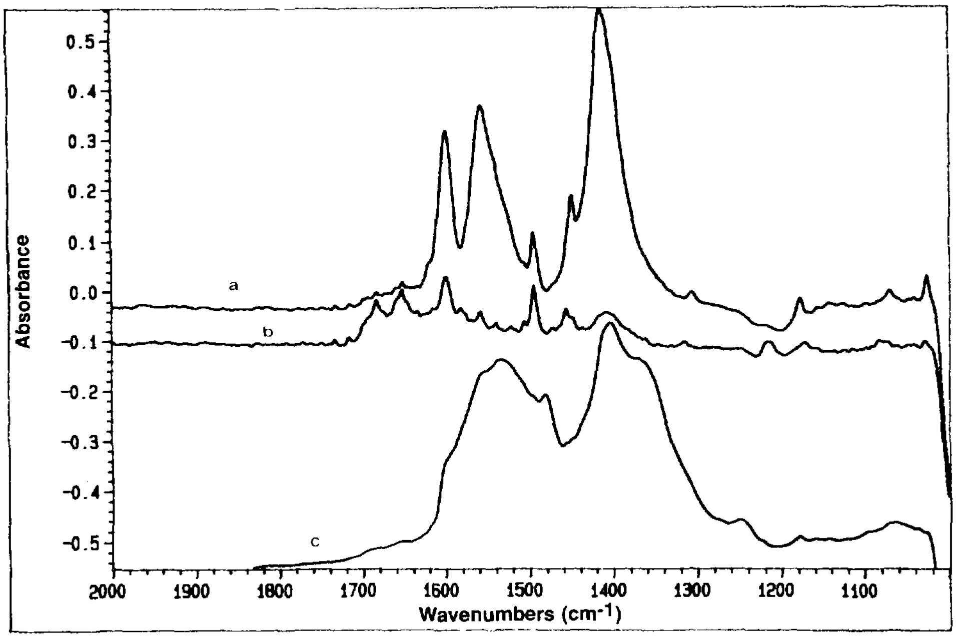

FIG. 9. FTIR spectra of the species arising from toluene oxidation over $MgCr_2O_{4-x}$ and successive evacuation at 483 (a) and 423 K (b); FTIR spectrum of the species arising from benzene oxidation over the same surface at 623 K (c). The spectrum of the activated catalyst disk has been automatically subtracted.

K. The most evident products are benzoate species, characterized by the asymmetric and symmetric COO stretchings at 1560 and 1413 cm^{-1} and by ring vibrations at 1598, 1495, 1448, 1305, 1180, 1065, and 1020 cm^{-1}, in agreement with Refs. (23 and 24). However, at 423 K two additional bands at 1684 and 1653 cm^{-1}, certainly due to the C=O stretchings, and at 1457, 1315, 1213, and 1171 cm^{-1} are observed: they correspond to typical bands of adsorbed benzaldehyde (24, 25).

The data concerning oxidation of benzene and toluene agree with the higher reactivity of C–H benzylic groups, similar to that of allylic C–H bonds of propene and 1-butene, and with the much lower reactivity of aromatic ring C–H bonds with respect to aliphatic saturated C–H bonds (except those of methane, which are extraordinarily inactive).

DISCUSSION

a. The Activation of Hydrocarbons on the $MgCr_2O_4$ Combustion Catalyst

Our data show that the hydrocarbons studied are oxidized by the surface of $MgCr_2O_{4+x}$, giving rise to adsorbed partial oxidation products, which later are more deeply oxidized, giving rise finally to carbon oxides (Scheme 1). The temperatures at which these reactions are observed are lower than or at most similar to those at which it behaves, like chromia (8) and other chromites (7, 9), as deep oxidation catalysts for hydrocarbons. The interaction of the catalyst with the more reactive hydrocarbons (1-butene, propene, isobutane) shows clearly, among the oxidation products, the formation of alkoxides (but-3-en-2-oxides, allyl alkoxides, and isobutoxides, respectively), i.e., the products of the breaking of a C–H bond of the hydrocarbon and of the corresponding production of a C–O single bond. When possible, these alk-

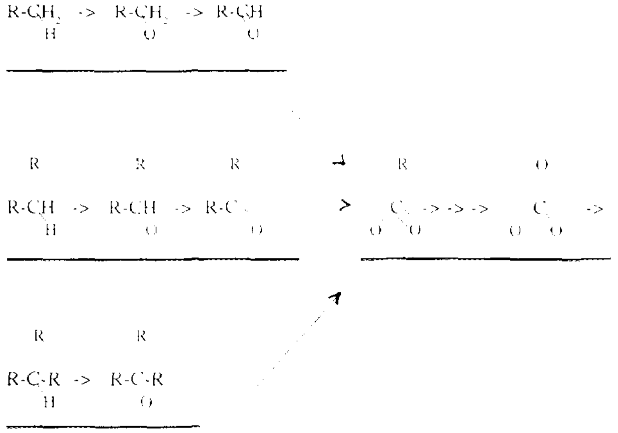

SCHEME 1. Proposed oxidation pathways for molecules activated at primary (methane, ethane, propene, toluene), secondary (propane, n-butane, 1-butene), and tertiary carbon (isobutane).

oxides are later oxidatively dehydrogenated, giving rise to carbonyl compounds (methyl vinyl ketone and acrolein from 1-butene and propene, respectively), while in the case of *ter*-butoxides (that cannot be further dehydrogenated at C_2), oxidative C–C bond cleavage is observed.

With less reactive hydrocarbons the alkoxides are not observed, but carbonyl compounds are directly seen. This is the case of acetone from propane, 2-butanone from *n*-butane, benzaldehyde from toluene, and probably (this is not proved here) acetaldehyde from ethane. In the case of the least reactive hydrocarbon, methane, CO_2 and carbonates (and water) are the only observed products; from benzene carboxylates arising from ring breaking are obtained.

This behaviour is understood if one takes into account that the overoxidation temperature of the partial oxidation surface products (alkoxides, carbonyl compounds, carboxylates) is similar in all cases while the activation temperature of the C–H bonds of the different hydrocarbons differs significantly. So, with the most reactive hydrocarbons, activated already at 300–423 K, all intermediates can be found. In contrast, with the less reactive hydrocarbons the activation step (C–H bond breaking) occurs at such a high temperature that all or some of the intermediates are already overoxidized and, correspondingly, cannot be detected.

Indeed, the temperature at which the oxidized products become detectable is rather well correlated with the energy for C–H bond dissociation, as summarized in Table 1; so, weaker C–H bonds are cleaved at lower temperatures, with few exceptions. The easier reaction observed with benzene with respect to methane (in contrast to the lower E_{dis} of the latter) can be explained assuming that unsaturated hydrocarbons (olefins and aromatics) interact molecularly more strongly with the surface and this could favour C–H bond scission. On the other hand, the interaction of localized π-type orbitals (those of olefins) can be stronger with respect to that of delocalized π-type orbitals. This can explain the slightly lower reactivity observed for toluene with respect to propene and 1-butene.

TABLE 1

C–H Bond Dissociation Energies and Threshold Oxidation Temperature of Hydrocarbons on $MgCr_2O_{4+x}$

Hydrocarbon	E_{diss} (kcal/mol)[a]	Threshold oxidation T (K)
C_6H_5–H	110	623
CH_3–H	104	773
CH_3–CH_2–H	98	473
$(CH_3)_2CH$–H	95	423
CH_3–CH_2–$(CH_3)CH$–H	≤95[b]	423
$(CH_3)_3C$–H	92	423
CH_2=CH–CH_2–H	88	373
C_6H_5–CH_2–H	85	423
CH_2=CH–$(CH_3)CH$–H	<88[b]	300

[a] From Ref. (47).

[b] Our estimates.

According to this correlation, the position at which C–H bond cleavage occurs in every molecule is that of the weaker C–H bonds. This explains the activation at the secondary carbon of propane and *n*-butane, the activation at the tertiary carbon in the case of isobutane, and the activation at allylic positions in the cases of propene and 1-butene and at benzylic position in the case of toluene. Interestingly, this leads to a completely different oxidation way in the cases of alkanes with respect to the corresponding alkenes (that are activated at different positions), as discussed previously in the case of propane and propene oxidation (6).

In conclusion, the present data strongly support the idea that the interaction of hydrocarbons with the catalyst surface occurs with breaking of the weaker C–H bond with the corresponding formation of a C–O bond, giving rise to an alkoxide. These alkoxides later undergo further oxidation giving, when possible, carbonyl compounds and, even later, carboxylate species as the result of oxidation of aldehydes or C–C bond breaking on ketones.

This viewpoint agrees with that arising from the data reported by Boreskov (26) that showed that the logarithm of the paraffin combustion rate over cuprous oxide linearly correlates with the C–H bond energy. Boreskov also reported that the oxidation rates for light hydrocarbons follows the trend olefines > aromatics > paraffins (26). We obtained similar trends with a different technique, which allowed us also to propose a detailed molecular mechanism, and using a different transition metal oxide catalyst. The carboxylate species, already recognized as intermediates in hydrocarbon catalytic combustion on metal oxides (26–28), are very evident due to their relatively high stability and to the strong intensity of their IR bands, but they are only final intermediates.

b. On the Mechanism of Catalytic Combustion on Transition Metal Oxides

The present data, obtained on a combustion catalyst, strongly support the previous proposal by our group (29), based on experiments carried out on selective oxidation catalyst, that unselective ways are essentially consecutive to both selective oxidation and oxy-dehydrogenation paths. In fact, we show here that at the surface of this combustion catalyst, light alkanes and alkenes as well as aromatics produce adsorbed partial oxidation compounds. These species are formed in the absence of dioxygen (either gas-phase or adsorbed), totally at the expense of the oxidized catalyst surface sites. So, the present data, according also to those previously published on the same catalytic system (6), support the idea that hydrocarbon total oxidation over this combustion catalyst occurs with the intermediacy of absorbed selective oxidation products. So, we propose the following conclusions: (i) total oxidation on transition metal oxides can be consecutive to partial oxidation; (ii) the same oxygen species (nucleophilic oxygen, i.e., O^{2-} ions on oxidized cationic sites) can be involved in both partial and total oxidation; (iii) discrimination between partial and total oxidation mainly depends on whether desorption of the partial oxidation product is faster or slower than its overoxidation.

This view is also supported by the remark that efficient selective oxidation processes mostly involve very stable products where charges are largely delocalized, like unsaturated cyclic anhydrides (phthalic and maleic anhydride) and unsaturated aldehydes (acrolein) or nitriles (acrylonitrile) (1, 2). All these products can be obtained with high selectivities and yields probably because they are very stable to overoxidation, under the given conditions.

This picture is partially in disagreement with that of Haber (2, 30), which assigns selective oxidation to nucleophilic oxygen species (O^{2-} lattice oxide ions) and combustion to electrophilic oxygen (O$_2$, O$_2^-$, and O$_2^{2-}$). Our study confirms that lattice oxygen performs selective oxidation, but suggests that it can also be involved in nonselective combustion ways. This does not exclude the possibility that electrophilic oxygen is also involved (together with nucleophilic oxygen) in a different combustion way or, perhaps, in some particular steps over this or other catalysts.

A different view, apparently conflicting with that of Haber, has been recently reported by Kung and co-workers (31), who proposed the existence of a "selectivity determining step," where bifurcation between selective oxy-dehydrogenation path and oxygen-containing compound production (including combustion) should occur on vanadia-based catalysts. According to Kung this bifurcation is related to the availability (or not) of bridging V–O–V oxygens. In contrast to both, Oyama *et al.* (32) proposed that bifurcation between selective dehydrogenation and combustion on vanadia catalysts occurs starting from two different adsorbed hydrocarbon species on the same sites.

Our viewpoint is somewhat in agreement with that of Kung, because the evolution of alkoxides (either towards the olefin, by elimination, or towards the ketones, by dehydrogenation) can just play the role of a "selectivity determining step" over some systems like, for example, Mg vanadates oxy-dehydrogenation catalysts (29, 32).

c. On the C–H Cleavage Step on Transition Metal Oxide Surfaces

The above view implies that the hydrocarbons are activated towards both selective and total oxidation by C–H bond cleavage. This cleavage necessarily occurs, in our system as well as on other transition metal oxides, at a reducible cation–oxide anion couple. The results of this interaction necessarily are: (i) one hydrogen leaves as an H$^+$ on the surface and probably links to an oxide ion giving rise to an hydroxy group; (ii) the alkyl group links to another oxide ion, giving rise to an alkoxy group; (iii) two electrons are assumed by the cation that is consequently reduced (Scheme 2). However, this result can be obtained in different ways, two of which are the simplest; (i) the primary interaction of the C–H bond occurs at surface oxide ions, via the interaction of the nonbonding orbitals of surface O^{2-} oxide species with the C–H σ^* antibonding orbitals of the hydrocarbon molecule, as proposed by different authors (2, 30, 33–35); (ii) the primary interaction of the C–H bond occurs at surface coordinatively unsaturated transition metal reducible cations.

The first model seems indeed to be very reasonable. However, the higher the electron density at surface oxide anions the higher the surface basicity. This should imply that activation of hydrocarbons should be favoured on basic catalysts, and should occur heterolytically, giving rise to alkyl anions (that are later oxidized to alkoxy groups). This view has been recently supported (36). However, although strong solid bases are certainly active in breaking C–H bonds (37), this can also occur (and much better) at the surface of solid acids. It is well known that solid Lewis acids are active in alkane isomerization (37), like *n*-butane to isobutane transposition. On sulphated zirconia, recently Pinna *et al.* (38) elegantly demonstrated that this reaction occurs at Lewis acid sites.

Accordingly, some of us related the catalytic activity in alkane oxidation over vanadia-based catalysts to the Lewis acidity of surface vanadium centers (29, 39, 40). This implies the interaction of C–H bonds with the surface cations instead of the anions. Moreover, in the case of MgCr$_2$O$_4$, as shown previously (6), and of chromia and

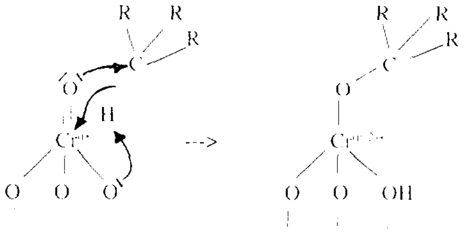

SCHEME 2. Proposed mechanism of C–H bond cleavage at the surface chromate sites of MgCr$_2$O$_{4-x}$.

other metal chromites, the surface seems to have a predominantly acid character, with weak basicity.

On the other hand, the ability of reduced metal centers to interact with C–H hydrocarbon bonds via hydrogen bondings (41) and to cause C–H bond breaking by "oxidative addition" (42) is well-known. These interactions are thought to primarily involve overlapping of *d* orbitals of the metal with σ and σ^* orbitals of the C–H bond. These overlappings cause the breaking of the C–H bond and the formation of C–M and M–H new bonds (oxidative addition).

The possibility of the interaction of C–H bonds with surface cations (in high oxidation state) in the case of metal oxide surfaces was proposed earlier, on spectroscopic bases, by Sheppard and co-workers (43). An interaction of C–H methane bonds with Mg^{2+} ions has been demonstrated recently even on a very basic surface such as MgO (44). Moreover, the overlapping of full and empty *d* orbitals of some transition metal cations with empty π^* and full π-type orbitals of olefins is well substantiated too by the formation of the so-called π complexes of olefins with cations like Pt^{2+}, Fe^{3+}, Cu^+, and Cr^{3+}, both on surfaces and in homoeneous complexes (28, 45). Similar complexes, although labile, have also been observed with d_0 cations like Ti^{4+} and Zr^{4+} (45, 46).

We propose here that C–H bond breaking on metal oxides can occur via direct interaction of σ and σ^* C–H orbitals with *d*-type orbitals of transition metal cations. This interaction is generally too weak to allow the detection of the molecular interacting species, but can be invoked to explain the mechanism of C–H bond breaking on metal oxides. The oxidizing metal centers tend to assume the couple of electrons, giving rise, with the cooperation of nearer oxide anions, to metal alkoxide and H^+ ions (Scheme 2).

This scheme seems to us to be reasonable in view of the known experimental data on alkane activation on metal oxides, and implies a direct electron flow between the oxidant (the cation) and the reducing agent (the hydrocarbon) without the intermediacy of the oxide anions. This scheme, which should be taken as a tentative one, emphasizes the role of coordinatively unsaturated cations in a Mars–van Krevelen-type mechanism (17) for both selective and unselective oxidation catalysis on transition metal oxides.

CONCLUSIONS

The conclusions of this work are as follows:

(i) Hydrocarbon C–H bonds are cleaved at the surface of an oxidized $MgCr_2O_{4+x}$ catalyst at $Cr^{n+}{=}O$ sites (n = 6 or 5), giving rise to alkoxy groups and reduced $Cr^{(n-2)+}$ centers.

(ii) These alkoxides are later further oxidized, giving rise to carbonyl compounds and/or carboxylate species that later burn to CO and CO_2.

(iii) In every hydrocarbon molecule, the C–H bonds broken first are those characterized by lower dissociation energy.

(iv) The rate of C–H bond cleavage on different hydrocarbons depends inversely on the C–H dissociation energy of the weakest C–H bond.

(v) The discussion of these data with previous data concerning hydrocarbon activation and oxidation on different catalysts allowed us to propose that hydrocarbon catalytic combustion on this transition metal oxide combustion catalyst consists in a series of reactions predominantly successive to partial oxidation reactions, with nucleophilic oxide ions as the active oxygen species.

(vi) A mechanism of C–H bond activation on transition metal oxides implying direct interaction of the C–H bonds with coordinately unsaturated transition metal cations is proposed.

ACKNOWLEDGMENTS

This work has been supported in part by MURST (Rome, Italy) and by NATO (CRG 900463).

REFERENCES

1. McKetta, J. J., Ed., "Chemical Processing Handbook," Dekker, New York, 1993.
2. Bielanski, A., and Haber, J., "Oxygen in Catalysts," Dekker, New York, 1991.
3. Wittcoff, H. A., CHEMTECH **20,** 48 (1990).
4. Silver, R. G., Sawyer, J. E., and Summers, J. C., Eds., "Catalytic Control of Air Pollution." American Chemical Society, DC, 1992.
5. Spivey, J. J., *Ind. Eng. Chem. Res.* **26,** 2165 (1987); *in* "Catalysis," Vol 8., p. 157. Royal Society of Chemistry, London, 1989.
6. Finocchio, E., Busca, G., Lorenzelli, V., and Willey, R. J., *J. Chem. Soc., Faraday Trans.*, accepted for publication.
7. Margolis, L. Ya., *Adv. Catal.* **14,** 429 (1963).
8. Yu Yao, Y., *J. Catal.* **28,** 139 (1974).
9. Terlecki-Baricevic, A., Grbic, B., Jovanovic, D., Angelov, S., Mehandziev, D., Morinova, C., and Kirilov-Stefanov, P., *Appl. Catal.* **47,** 145 (1989).
10. Carberry, J. J., Rajadurai, S., Alcock, C. B., and Li, B., *Catal. Lett.* **4,** 43 (1990).
11. Willey, R., Noirclerk, P., and Busca, G., *Chem. Eng. Commun.* **123,** 1 (1993).
12. Hubbard, C. P., Otto, K., Gandhi, H. S., and Ng, K. Y. S., *J. Catal.* **144,** 484 (1993).
13. Barnard, K. R., Foger, K., Tunney, T. W., and Williams, R. D., *J. Catal.* **125,** 265 (1990).
14. Bart, J. M., Pentenero, A., and Prigent, M. F., in "Catalytic Control of Air Pollution" (R. G. Silver, J. E. Sawyer, and J. C. Summers, Eds.), p. 42. American Chemical Society, Washington, DC, 1992.
15. Klissurski, D., Hadjiivanov, H., and Davydov, A. A., *J. Catal.* **111,** 421 (1988).
16. Shimizu, Y., Kusano, S., Kuwayama, H., Tanaka, K., and Egashira, K., *J. Am. Ceram. Soc.* **73,** 818 (1990).

17. Mars, P., and Van Krevelen, D. W., *Chem. Eng. Sci.* **3,** 41, (1954).
18. Busca, G., and Lorenzelli, V., *Mater. Chem.* **7,** 89, (1982).
19. Busca, G., Lamotte, J., Lavalley, J. C., and Lorenzelli, V., *J. Am. Chem. Soc.* **109,** 4197 (1987).
20. Lynch, C. T., Mazdiyasni, K. S., Smith J. S., and Crawford, J., *Anal. Chem.* **36,** 2332 (1964).
21. Ramis, G., Busca, G., and Lorenzelli, V., *J. Chem. Soc., Faraday Trans. 1* **83,** 1591 (1987).
22. Bowles, A. J., George, W. O., and Maddams, W. F., *J. Chem. Soc. B* 810 (1969); Krantz, A., Goldfarb, T. D., and Lin, C. Y., *J. Am. Chem. Soc.* **94,** 4022 (1972).
23. Green, J. H. S., *Spectrochim. Acta, Part A* **33,** 575 (1977).
24. Busca, G., Cavani, F., and Trifirò, F., *J. Catal.* **106,** 471 (1987).
25. Green, J. H. S., and Harrison, D. T., *Spectrochim. Acta, Part A* **32,** 1265 (1976).
26. Boreskov, G. K., *in* "Catalysis Science and Technology" (J. R. Anderson and M. Boudart, Eds.), Vol. 3, p. 39. Springer-Verlag, New York, 1982.
27. Kuznetsov, V. A., Gerei, S. V., and Gorokhovatskii, Ya. B., *Kinet. Katal.* **18,** 710 (1977).
28. Davydov, A. A., *in* "Infrared Spectroscopy of Adsorbed Species on the Surface of Transition Metal Oxides," p. 195. Wiley, New York, 1990; Davydov, A. A., Mikhaltchenko, V. G., Sokolvskii, V. D., and Boreskov, G. K., *J. Catal.* **55,** 299 (1978).
29. G. Busca, V. Lorenzelli, G. Oliveri, and G. Ramis, *in* "New Developments in Selective Oxidation" (V. Cortes Corberan and S. Vic Bellon, Eds.), p. 253. Elsevier, Amsterdam, 1994.
30. Haber, J., *in* "Catalysis of Organic Reactions" (J. R. Kosak and T. A. Johnson, Eds.), p. 151. Dekker, 1994.
31. Michalakos, P. M., Kung, M. C., Jahan, I., and Kung, H. H., *J. Catal.* **140,** 226 (1993).
32. Oyama, S. T., Desikan, A. N., and Zhang, W., *in* "Catalytic Selective Oxidation" (S. T. Oyama and J. W. Hightower, Eds.), p. 16. American Chemical Society, Washington, DC, 1993.
33. Haber, J., Tokarz, R., and Witko, M. *in* "New Developments in Selective Oxidation" (V. Cortes Coberan and S. Vic Bellon, Eds.), p. 739. Elsevier, Amsterdam, 1994.
34. Haber, J., *in* "Structure and Reactivity of Surfaces" (C. Morterra, A. Zecchina, and G. Costa, Eds.), p. 447. Elsevier, Amsterdam, 1989.
35. Ziolkowski, J., Bordes, E., and Courtine, P., *in* "New Developments in Selective Oxidation" (G. Centi and F. Trifirò, Eds.), p. 625. Elsevier, Amsterdam, 1990.
36. Mamedov, E. A., Vilovskii, V. P., Talyshinskii, R. M., and Rizayev, R. G. *in* "Studies in Surface Science and Catalysis" (P. Ruiz and B. Delmon, Eds.), Vol. 72, p. 379. Elsevier, Amsterdam, 1992.
37. Tanabe, K., Misono, M., Ono, Y., and Hattori, H., "New Solid Acids and Bases," Elsevier, Amsterdam, 1989.
38. Pinna, F., Signoretto, M., Strukul, G., Cerrato, G., and Morterra, C., *Chem. Lett.* **26,** 339 (1994).
39. Busca, G., Centi, G., and Trifirò, F., *J. Am. Chem. Soc.* **107,** 7757 (1985).
40. Busca, G., Centi, G., Trifirò, F., and Lorenzelli, V., *J. Phys. Chem.* **90,** 1337 (1986).
41. Demuth, J. E., Ibach, H., and Lehwald, S., *Phys. Rev. Lett.* **40,** 1044 (1978); Trofimenko, S., *J. Am. Chem. Soc.* **89,** 6288 (1967).
42. Albert, M. R., and Yates, J. T., "The Surface Scientist's Guide to Organometallic Chemistry." American Chemical Society, Washington, DC, 1987.
43. Al-Mashta, F., Davanzo, C. U., and Sheppard, N., *J. Chem. Soc., Chem. Commun.*, 1258 (1983).
44. Li, C., Li, G., and Xin, Q., *J. Phys. Chem.* **98,** 1933 (1994).
45. Busca, G., Lorenzelli, V., Ramis, G., and Sanchez Escribano, V., *Mater. Chem. Phys.* **29,** 175 (1991).
46. Busca, G., Ramis, G., Lorenzelli, V., Janin, A., and Lavalley, J. C., *Spectrochim. Acta, Part A* **43,** 489 (1987).
47. Morrison, R. T., and Boyd, R. N., "Organic Chemistry," 4th ed. Allyn and Bacon, Boston, 1983.